

# Shedding light on neutrino self-interactions with solar antineutrino searches

---

Quan-feng Wu<sup>a,b</sup> and Xun-Jie Xu<sup>a</sup>

<sup>a</sup>*Institute of High Energy Physics, Chinese Academy of Sciences, Beijing 100049, China*

<sup>b</sup>*School of Physical Sciences, University of Chinese Academy of Sciences, Beijing 100049, China*

*E-mail:* [wuquanfeng@ihep.ac.cn](mailto:wuquanfeng@ihep.ac.cn), [xuxj@ihep.ac.cn](mailto:xuxj@ihep.ac.cn)

ABSTRACT: Solar antineutrinos are absent in the standard solar model prediction. Consequently, solar antineutrino searches emerge as a powerful tool to probe new physics capable of converting neutrinos into antineutrinos. In this study, we highlight that neutrino self-interactions, recently gaining considerable attention due to their cosmological and astrophysical implications, can lead to significant solar antineutrino production. We systematically explore various types of four-fermion effective operators and light scalar mediators for neutrino self-interactions. By estimating the energy spectra and event rates of solar antineutrinos at prospective neutrino detectors such as JUNO, Hyper-Kamiokande, and THEIA, we reveal that solar antineutrino searches can impose stringent constraints on neutrino self-interactions and probe the parameter space favored by the Hubble tension.

---

## Contents

<b>1</b>	<b>Introduction</b>	<b>1</b>
<b>2</b>	<b>Four-fermion effective operators</b>	<b>2</b>
2.1	Solar antineutrino production	3
2.2	Calculation of solar antineutrino spectra	4
2.3	Neutrino flavors and neutrino oscillations	5
2.4	Event rates, $\chi^2$ analyses, and results	6
<b>3</b>	<b>Light mediators</b>	<b>8</b>
3.1	Opening up the effective vertices	8
3.2	Results	9
<b>4</b>	<b>Conclusion</b>	<b>10</b>
<b>A</b>	<b>Identities for Weyl, Dirac, and Majorana spinors</b>	<b>11</b>
<b>B</b>	<b>Calculation of three-body decay</b>	<b>12</b>
<b>C</b>	<b>Calculation of four- and five-body decay</b>	<b>14</b>

---

## 1 Introduction

The Sun, serving as the most intense natural source of neutrinos detected on Earth, provides a unique opportunity to investigate neutrino properties and probing underlying new physics [1, 2]. The standard solar model, combined with our current understanding of neutrinos, predicts that only neutrinos — not antineutrinos — can be emitted by the Sun. Consequently, the detection of solar antineutrinos would be compelling evidence of new physics, which has motivated numerous experimental efforts in the search for solar antineutrinos [3–8].

Theoretically, solar antineutrinos can be produced through neutrino-antineutrino oscillations [9, 10], which were considered as one of the potential solutions to the historical “solar neutrino missing problem” [11, 12]. This effect could be significant in the presence of large neutrino magnetic moments and the solar magnetic field [13–18]. In addition, solar antineutrinos might also be produced via neutrino decay or DM annihilation in the Sun — see e.g. [19–26].

In this work, we propose that neutrino self-interactions, which are challenging to probe in the laboratory [27–30] but have recently attracted significant attention due to their cosmological and astrophysical implications [30–48], might serve as another source of solar antineutrinos.

Consider, for instance, a four-neutrino effective operator  $\frac{1}{\Lambda^2}\nu^\dagger\nu^\dagger\nu\nu$ , where  $\nu$  denotes the two-component Weyl spinor of a neutrino and  $\Lambda$  is the cut-off energy scale. With this operator in play, a final-state neutrino in any process responsible for solar neutrino production can be substituted with one antineutrino and two neutrinos in the final state, implying the existence of an additional process for solar antineutrino production. More generally, for all possible Lorentz-invariant four-neutrino operators (e.g.,  $\nu\nu\nu\nu$ ,  $\nu^\dagger\bar{\sigma}_\mu\nu\nu^\dagger\bar{\sigma}^\mu\nu$ , etc.), we can argue that at least one antineutrino can be produced in similar processes.

Solar antineutrinos can be readily detected through inverse beta decay (IBD) which benefits from well-developed technology for both event identification and reconstruction. Given the advantages of IBD detection, we anticipate that next-generation neutrino detectors will exhibit substantially improved sensitivity to solar antineutrinos.

Therefore, in this work we investigate the potential of probing neutrino self-interactions through future solar antineutrino searches at JUNO [49], Hyper-Kamiokande (HK) [50], and THEIA [51]. As our results will show, solar antineutrino searches can provide the most competitive constraints on neutrino self-interactions within a certain range of parameter space. Notably, the parameter space proposed by Ref. [31] for resolving the Hubble tension will be fully probed by solar antineutrino searches.

This article is structured as follows: In Sec. 2, we formulate all possible four-fermion effective operators for neutrinos and relate them to solar antineutrino production. Then we calculate the fluxes of solar antineutrinos produced through these operators, take the oscillation effect into account, and determine the IBD event rates at neutrino detectors. In Sec. 3, we open up the effective vertices and investigate the impact of light mediators involved in neutrino self-interactions. Finally we conclude in Sec. 4 and relegate some details to the appendix.

## 2 Four-fermion effective operators

For neutrino self-interactions, we start from four-fermion effective operators. The most general Lorentz-invariant four-fermion operators that one can write down for Majorana<sup>1</sup> neutrinos are

$$\mathcal{L}_S = \frac{1}{\Lambda_S^2}(\nu\nu)(\nu\nu) + \text{h.c.}, \quad (2.1)$$

$$\mathcal{L}_{S'} = \frac{1}{\Lambda_{S'}^2}(\nu\nu)(\nu^\dagger\nu^\dagger), \quad (2.2)$$

$$\mathcal{L}_V = \frac{1}{\Lambda_V^2}(\nu^\dagger\bar{\sigma}^\mu\nu)(\nu^\dagger\bar{\sigma}_\mu\nu), \quad (2.3)$$

$$\mathcal{L}_{V'} = \frac{1}{\Lambda_{V'}^2}(\nu^\dagger\bar{\sigma}^\mu\nu)(\nu\sigma_\mu\nu^\dagger), \quad (2.4)$$

$$\mathcal{L}_T = \frac{1}{\Lambda_T^2}(\nu\sigma^{\mu\nu}\nu)(\nu\sigma_{\mu\nu}\nu) + \text{h.c.} \quad (2.5)$$

---

<sup>1</sup>In this work, we only consider Majorana neutrinos because Dirac neutrinos with strong self-interactions are severely constrained by cosmological  $N_{\text{eff}}$  [52, 53].

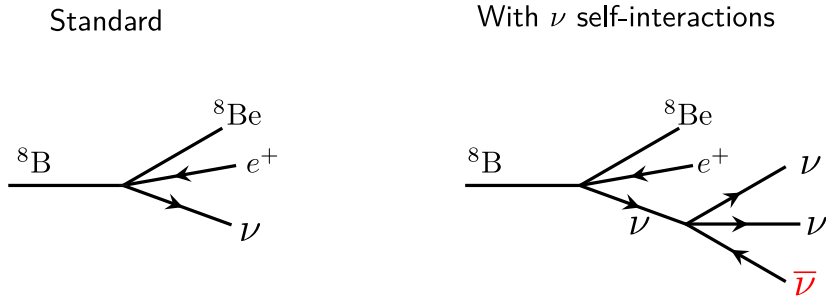


**Figure 1.** Production of solar neutrinos (left panel) and antineutrinos (right panel) from  ${}^8\text{B}$  decay in the presence of the  $(\nu\nu)(\nu^\dagger\nu^\dagger)$  operator.

Here we formulate the interactions using two-component Weyl spinors following the convention in Ref. [54], including for example  $\nu\nu \equiv \nu_a\nu^a$ ,  $\nu^\dagger\nu^\dagger \equiv \nu^{\dagger a}\nu_a^\dagger$ ,  $\sigma^\mu = (1, \vec{\sigma})$ ,  $\bar{\sigma}^\mu = (1, -\vec{\sigma})$ ,  $\sigma^{\mu\nu} \equiv \frac{i}{4}(\sigma^\mu\bar{\sigma}^\nu - \sigma^\nu\bar{\sigma}^\mu)$ , and  $\bar{\sigma}^{\mu\nu} \equiv \frac{i}{4}(\bar{\sigma}^\mu\sigma^\nu - \bar{\sigma}^\nu\sigma^\mu)$ . We adopt Weyl spinors for the purpose of showing the distinction between neutrinos and antineutrinos more explicitly. This approach can be conveniently transformed to the more commonly used formalism of Dirac spinors, as detailed in Appendix A. The four (anti-)neutrinos in Eqs. (2.1)-(2.5) may possess different flavors, which will be discussed in detail in Sec. 2.3.

In addition to Eqs. (2.1)-(2.5), one might consider the operator  $(\nu\sigma^{\mu\nu}\nu)(\nu^\dagger\bar{\sigma}_{\mu\nu}\nu^\dagger)$  but it vanishes according to the Fierz identities. Besides, one can show that  $\mathcal{L}_{S'}$  and  $\mathcal{L}_{V'}$  can be transformed to  $\mathcal{L}_V$ , and  $\mathcal{L}_T$  can be transformed to  $\mathcal{L}_S$ . These aspects are detailed in Appendix A.

## 2.1 Solar antineutrino production

Let us now consider the production of solar (anti)neutrinos. Solar neutrinos are produced from fusion of light elements (e.g.,  $p + p \rightarrow {}^2\text{H} + e^+ + \nu_e$ ) or decay of unstable elements created via fusion (e.g.,  ${}^8\text{B} \rightarrow {}^8\text{Be} + e^+ + \nu_e$ ). In the presence of operators like  $(\nu\nu)(\nu^\dagger\nu^\dagger)$ , solar antineutrinos can be generated from processes<sup>2</sup> that split one neutrino from the aforementioned reactions into three (anti)neutrinos, as depicted in Fig. 1. Obviously, one of them must be an antineutrino if the splitting is caused by the  $(\nu\nu)(\nu^\dagger\nu^\dagger)$  operator, which respects the lepton number conservation.

More generally, it is evident that other operators can also result in the production of at least one antineutrino. Actually, the operators  $(\nu\nu)(\nu\nu)$  and  $(\nu\sigma^{\mu\nu}\nu)(\nu\sigma_{\mu\nu}\nu)$  can produce three antineutrinos via analogous processes. One might speculate whether there could be operators consisting of one  $\nu$  and three  $\nu^\dagger$ 's, which would imply that the right diagram in Fig. 1 produces no antineutrinos. However, due to Lorentz invariance, this scenario is

<sup>2</sup>We note here that with the new processes involving neutrino self-interactions, nuclear fusion and decay rates in the Sun are also slightly changed, causing a small variation of energy production at the magnitude of  $\sim 10^{-5}$  for the typical self-interaction strength considered in this work. Given that the uncertainties in the density, temperature, and chemical composition profiles are much higher than this magnitude, such a variation is unlikely to be of observational importance.

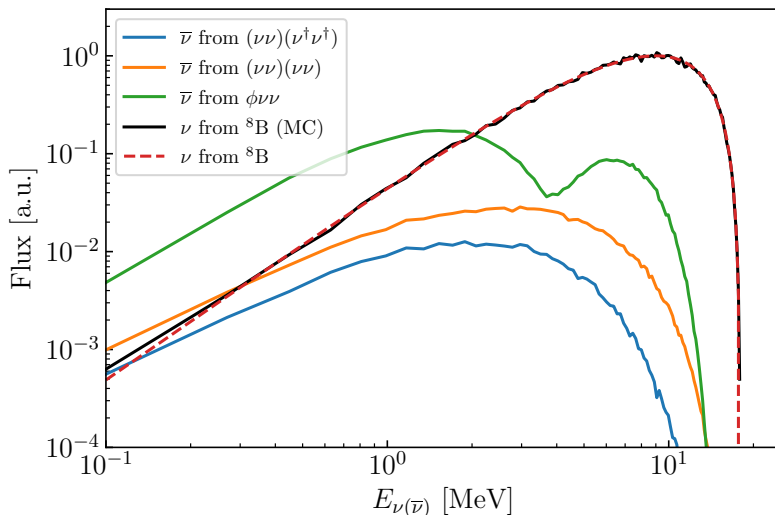


**Figure 2.** Energy spectra of solar  $\nu$  and  $\bar{\nu}$  from  ${}^8\text{B}$  decay. All solid curves are obtained using the Monte Carlo method. The dashed curve, which represents the standard  ${}^8\text{B}$  decay, is obtained from analytical calculation and has been normalized to unity at the peak. The new physics curves have been normalized by the same factor multiplied by  $10^4$ . The shown examples take  $\Lambda_S = \Lambda_{S'} = 10$  MeV and  $(m_\phi/\text{MeV}, g_\phi) = (12.6, 1)$ .

impossible. More specifically,  $\nu$  and  $\nu^\dagger$  are under the  $(\frac{1}{2}, 0)$  and  $(0, \frac{1}{2})$  representations of the Lorentz group  $\text{SO}(3, 1)$ , respectively, and there is no Lorentz-invariant operator composed of an odd number of fields that are under  $(\cdot, \frac{1}{2})$  representations where “ $\cdot$ ” stands for arbitrary integers or half-integers.

Hence, we conclude that any Lorentz-invariant four-neutrino effective interactions inevitably lead to the production of solar antineutrinos.

## 2.2 Calculation of solar antineutrino spectra

In this work, we only consider solar antineutrinos originating from  ${}^8\text{B}$  decay. In principle, pp fusion could, given the same self-interaction strength, produce a much higher antineutrino flux than  ${}^8\text{B}$  decay. However, the energy of an antineutrino produced via pp fusion ( $E_{\bar{\nu}} \lesssim 0.4$  MeV) is well below the threshold of IBD detection (1.8 MeV). So we do not consider the contribution of pp fusion.

The calculation of solar antineutrino spectra from  ${}^8\text{B}$  decay involves the Feynman diagram in the right panel of Fig. 1, which requires the integration of five-body phase space. To our knowledge, there is no simple analytical approach to this problem but some recursive relations (see e.g. Ref. [55]) can be used to facilitate numerical evaluations. We present the details in Appendix C and implement the algorithm in our code<sup>3</sup>. The code allows us to perform Monte Carlo integration of multi-body phase space efficiently.

Figure 2 shows the energy spectra of solar  $\nu$  and  $\bar{\nu}$  from  ${}^8\text{B}$  decay obtained using our Monte Carlo code. Note that for the standard process  ${}^8\text{B} \rightarrow {}^8\text{Be} + e^+ + \nu_e$  which is a three-

<sup>3</sup>Our code is publicly accessible via <https://github.com/Fenyutanchan/solar-vSI>.

body decay, the energy spectrum can also be computed analytically — see Appendix B. This is plotted in Fig. 2 as the red dashed curved. As is shown in the figure, the Monte Carlo result of computing the standard  ${}^8\text{B}$  decay (black curve) agrees well with the analytical result.

In the presence of neutrino self-interactions, the antineutrino fluxes from  ${}^8\text{B}$  decay are shown by the blue, orange, and green curves, for  $(\nu\nu)(\nu^\dagger\nu^\dagger)$ ,  $(\nu\nu)(\nu\nu)$ , and  $\phi\nu\nu$ , respectively. The interaction  $\phi\nu\nu$ , together with the double-peak structure of the flux, will be discussed in Sec. 3. The flux for  $(\nu\nu)(\nu\nu)$  is higher than the flux for  $(\nu\nu)(\nu^\dagger\nu^\dagger)$ . This is because  $(\nu\nu)(\nu\nu)$  converts one neutrino to three antineutrinos while  $(\nu\nu)(\nu^\dagger\nu^\dagger)$  can only produce one antineutrino.

Here we would like to discuss an additional contribution to the antineutrino flux. Given that neutrinos have three mass eigenstates and the lightest one can be arbitrarily light, it is possible that a relatively heavy neutrino state among them can decay into three lighter ones due to the  $4\nu$  self-interactions. Such decays could also produce antineutrinos. However, due to the highly suppressed decay rates, this part of contribution is negligible, as can be seen from the following estimate. For a mass eigenstate with mass  $m_\nu$  decaying to three massless states, the decay rate can be estimated by analogy with the decay of muon<sup>4</sup>:

$$\Gamma_{\nu \text{ decay}} \sim \frac{\Lambda^{-4} m_\nu^5}{192\pi^3} \sim \frac{1}{4 \times 10^{17} \text{sec}} \left( \frac{\text{MeV}}{\Lambda} \right)^4 \left( \frac{m_\nu}{0.1 \text{eV}} \right)^5, \quad (2.6)$$

which implies that the corresponding lifetime is almost as long as the age of the universe ( $4.35 \times 10^{17}$  sec) if  $\Lambda = 1$  MeV and  $m_\nu = 0.1$  eV. Taking this as a benchmark value, the probability of a neutrino decaying before it arrives at Earth is

$$P_{\nu \text{ decay}} \sim \Gamma_{\nu \text{ decay}} L_\odot \frac{m_\nu}{E_\nu} \sim 10^{-23}, \quad (2.7)$$

where  $L_\odot = 1.471 \times 10^8$  km is the distance from Earth to the Sun, and  $m_\nu/E_\nu \sim 10^{-8}$  accounts for the relativistic time dilation effect. Eq. (2.7) implies that the antineutrino flux produced via neutrino decays is highly suppressed compared to those presented in Fig. 2, hence negligible in our analysis.

### 2.3 Neutrino flavors and neutrino oscillations

We can generally assign different flavors to the (anti)neutrino fields in Eqs. (2.1)-(2.5), e.g.,  $(\nu^\dagger \bar{\sigma}^\mu \nu)(\nu^\dagger \bar{\sigma}_\mu \nu) \rightarrow (\nu_\alpha^\dagger \bar{\sigma}^\mu \nu_{\alpha'}) (\nu_\beta^\dagger \bar{\sigma}_\mu \nu_{\beta'})$ . Correspondingly, we add flavor indices to the  $\Lambda$ 's, e.g.,  $\Lambda_V^2 \rightarrow \Lambda_{V\alpha\alpha'\beta\beta'}^2$ . Among the various flavorful operators, only those with at least one  $\nu_e$  are relevant to our analysis. So we only consider such operators and, without loss of generality, we take  $\alpha' = e$ .

The flavorful operators imply that antineutrinos being produced from them may not necessarily be  $\bar{\nu}_e$ . They can be  $\bar{\nu}_\mu$  or  $\bar{\nu}_\tau$ . Due to the standard neutrino oscillation, they may be converted to  $\bar{\nu}_e$  when arriving at the Earth. Note that the standard neutrino oscillation can change the flavor composition, but not the composition of  $\nu$  and  $\bar{\nu}$ .

<sup>4</sup>The muon decay rate is approximately given by  $\Gamma_\mu \approx G_F^2 m_\mu^5 / 192\pi^3$  if all final state masses are neglected.

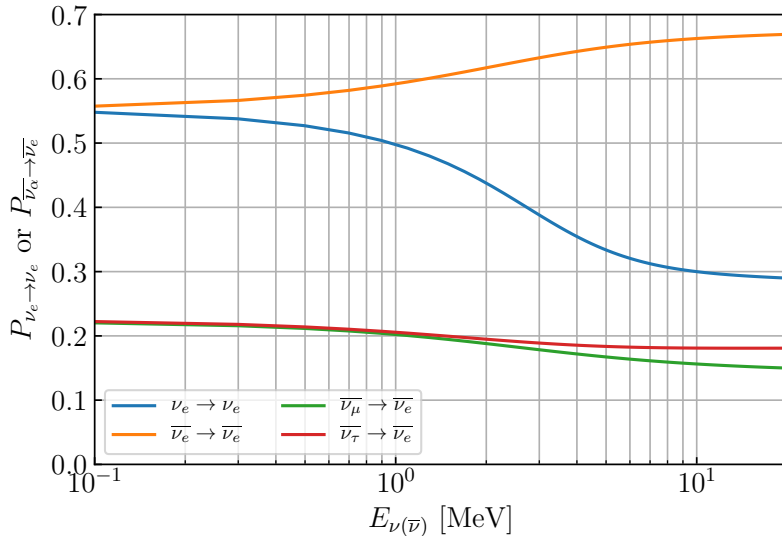


**Figure 3.** Solar neutrino oscillation probabilities for  $\nu_e \rightarrow \nu_e$  and  $\bar{\nu}_\alpha \rightarrow \bar{\nu}_e$ .

To account for the flavor conversion caused by neutrino oscillation, we adopt the adiabatic approximation following the prescription in Ref. [2] and calculate the conversion probabilities of antineutrinos. The oscillation parameters used in our calculation are [56, 57]:

$$(\theta_{12}, \theta_{13}, \theta_{23}, \delta_{\text{CP}}) = (33.41^\circ, 8.54^\circ, 49.1^\circ, 0), \quad (2.8)$$

$$(\Delta m_{21}^2, \Delta m_{31}^2) = (7.4 \times 10^{-5}, 2.5 \times 10^{-3}) \text{eV}^2. \quad (2.9)$$

The result is illustrated in Fig. 3. For  $\nu_e \rightarrow \nu_e$ , the oscillation probability at the high-energy end of the curve is approximately  $\sin^2 \theta_{12} \approx 0.3$ . But for  $\bar{\nu}_e \rightarrow \bar{\nu}_e$ , the probability can be significantly higher, because antineutrinos flip the sign of the MSW potential, resulting in  $P_{\bar{\nu}_e \rightarrow \bar{\nu}_e} \approx \cos^2 \theta_{12} \approx 0.7$ . If the antineutrinos are initially produced as  $\bar{\nu}_\mu$  or  $\bar{\nu}_\tau$ , neutrino oscillation can still convert  $\sim 20\%$  of them to  $\bar{\nu}_e$  according to Fig. 3. Note that, unlike  $\nu_e \rightarrow \nu_e$  or  $\bar{\nu}_e \rightarrow \bar{\nu}_e$ , the flavor transition probabilities  $P_{\bar{\nu}_\mu \rightarrow \bar{\nu}_e}$  and  $P_{\bar{\nu}_\tau \rightarrow \bar{\nu}_e}$  depend on the CP phase  $\delta_{\text{CP}}$  which is largely unknown. For neutrinos, the effect of the CP phase on  $P_{\nu_e \rightarrow \nu_\alpha}$  ( $\alpha \neq e$ ) is known to be significant, typically varying  $P_{\nu_e \rightarrow \nu_\alpha}$  by  $50\% \sim 70\%$  [58]. In the case of antineutrinos, our analysis reveals that this impact is considerably milder, confined to roughly  $\sim 10\%$ . Hence, the influence of the CP phase can be disregarded in our analysis.

#### 2.4 Event rates, $\chi^2$ analyses, and results

By combing the Monte Carlo integration presented in Fig. 2 and the oscillation probabilities in Fig. 3, it is straightforward to compute the solar  $\bar{\nu}_e$  flux arriving at the Earth. Then we compute the event rates at three future neutrino detectors, namely JUNO [49], Hyper-Kamiokande (HK) [50], and THEIA [51]. We consider the IBD detection channel which is only sensitive to  $\bar{\nu}_e$ . The event rates are computed via

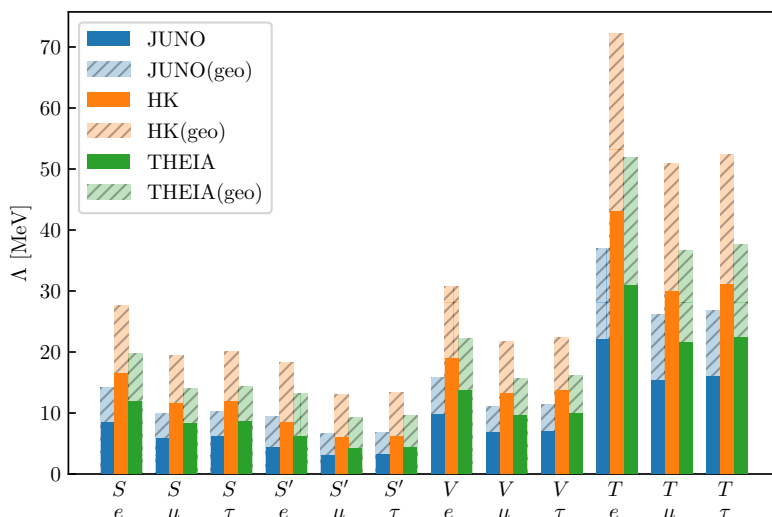


**Figure 4.** The sensitivity reach of future experiments in probing the four-fermion operators of neutrino self-interactions, at the 90% C.L. The  $x$ -axis labels ( $S$ ,  $S'$ ,  $V$ ,  $T$ ) indicate the type of the operators — see Eqs. (2.1)-(2.5), and ( $e$ ,  $\mu$ ,  $\tau$ ) indicate the flavor of the antineutrino being produced from  ${}^8\text{B}$  decay. The bars in solid colors include reactor neutrinos and geoneutrinos as backgrounds; the hatched bars in lighter colors assume the reactor-off scenario, in which geoneutrinos become the dominant background.

$$\frac{dN}{dE_\nu} = N_{\text{H}} \Delta t \sigma_{\text{IBD}}(E_\nu) \phi_{\bar{\nu}_\alpha}(E_\nu) P_{\bar{\nu}_\alpha \rightarrow \bar{\nu}_e}(E_\nu), \quad (2.10)$$

where  $N_{\text{H}}$  denotes the number of hydrogen atoms in the detector,  $\Delta t$  is the exposure time,  $\sigma_{\text{IBD}}$  is the cross section of IBD with a threshold of 1.8 MeV, and  $\phi_{\bar{\nu}_\alpha}$  denotes the flux of  $\bar{\nu}_\alpha$ . For  $\sigma_{\text{IBD}}$ , we adopt the calculations in [59]. The exposure time is universally assumed to be 10 years for all detectors.  $N_{\text{H}}$  is computed from the fiducial mass of the detector, which for JUNO, HK, and THEIA is 20, 187, and 100 kilo-tons, respectively. Since JUNO is a liquid scintillator detector, we assume that the chemical composition is  $\text{C}_n\text{H}_{2n}$ , in contrast to the other two water-based ( $\text{H}_2\text{O}$ ) detectors.

To quantitatively evaluate the experimental sensitivity to neutrino self-interactions, we adopt the following binned  $\chi^2$  function [60]:

$$\chi^2 = \sum_i 2 \left( \mu_i - n_i + n_i \log \frac{n_i}{\mu_i} \right), \quad (2.11)$$

where  $\mu_i$  and  $n_i$  denote, respectively, the expected and observed numbers of events in the  $i$ -th energy bin. Eq. (2.11) allows us to readily include backgrounds, which should be added to the signal as follows:

$$\mu_i = \mu_i^{\nu\text{SI}} + \mu_i^{\text{bkg}}, \quad (2.12)$$

where  $\mu_i^{\nu\text{SI}}$  and  $\mu_i^{\text{bkg}}$  denote the contributions of neutrino self-interactions and backgrounds, respectively.



For solar antineutrino searches, the backgrounds mainly come from reactor neutrinos and geoneutrinos. Other backgrounds such as the diffuse supernova neutrino background (DSNB) and atmospheric neutrinos within the energy range of interest are several orders of magnitude lower so they are neglected in our analysis. For the reactor neutrino background, we take the spectral shape from Ref. [61] and the total fluxes, which are location-dependent, from Refs. [2, 62]. For geoneutrinos, we assume a universal flux for all experiments, taken from Ref. [63]. Note that the reactor neutrino background depends on the operational status of nearby reactors. It is possible that the experiments may be able to collect a long period of reactor-off data, either continuously or cumulatively, which would feature a substantially reduced reactor neutrino background. To demonstrate the impact of this reduction, we also present results without including the reactor background so that geoneutrinos become the dominant background. These are denoted by “geo” in the labels in Fig. 4.

When using Eq. (2.11) to evaluate the experimental sensitivity, we set limits at the 90% C.L., corresponding to  $\Delta\chi^2 = 2.71$  [60], where  $\Delta\chi^2$  is the difference of the two  $\chi^2$  values with and without neutrino self-interactions.

Our analyses for four-fermion effective operators are presented in Fig. 4. The heights of the bars in Fig. 4 indicate the value of  $\Lambda$  required to generate one IBD event at the detector. In each instance, we consider only one type of the operators, which can be  $S$ ,  $S'$ ,  $V$ , or  $T$  according to Eqs. (2.1)-(2.5). Results for  $V'$  operators are not presented since they are identical to the results for  $V$ . The flavor labels ( $e$ ,  $\mu$ ,  $\tau$ ) on the  $x$ -axis indicate the initial flavor of the produced antineutrinos. For simplicity, we assume that the antineutrinos originating from  ${}^8\text{B}$  decay are only of a single flavor. It is possible that multi-flavor antineutrinos could be produced from one operator. For instance, antineutrinos with the flavor composition  $\bar{\nu}_e + \bar{\nu}_\mu + \bar{\nu}_\tau$  can be produced from the operator  $(\nu_\mu\nu_e)(\nu_e\nu_\tau)$ . In this case, one needs to sum over the flavor index  $\alpha$  in Eq. (2.10).

As is shown in Fig. 4, solar antineutrino observations in future experiments might shed light on neutrino self-interactions with  $\Lambda$  at  $\sim 10$  MeV or even higher, depending on the flavor and the type of interactions. This is to be compared with the self-interaction strength favored by the Hubble tension in cosmology [27, 31]:

$$\Lambda_{H_0 \text{ tension}} = \begin{cases} 4.6 \pm 0.5 \text{ MeV} & \text{(SI)} \\ 90_{-60}^{+170} \text{ MeV} & \text{(MI)} \end{cases}, \quad (2.13)$$

where SI and MI indicates the “strongly interacting” (SI) or “moderately interacting” (MI) regimes considered in Ref. [31]. We see that future solar antineutrino observations can fully probe the SI regime and in some cases even enter the MI regime.

### 3 Light mediators

#### 3.1 Opening up the effective vertices

As the order of magnitude of  $\Lambda$  considered in the above analysis is typically around ten or a few tens of MeV, we should consider how such operators might open up at energy scales

comparable to  $\Lambda$ . The simplest possibility would be adding a scalar ( $\phi$ ) or vector ( $A_\mu$ ) mediator such as

$$(\nu\nu)(\nu\nu) \rightarrow \overline{(\nu\phi\nu)(\nu\phi\nu)} \quad \text{or} \quad (\nu^\dagger\bar{\sigma}^\mu\nu)(\nu^\dagger\bar{\sigma}_\mu\nu) \rightarrow (\nu^\dagger\bar{\sigma} \cdot A\nu)(\nu^\dagger\bar{\sigma} \cdot A\nu). \quad (3.1)$$

In addition, the four-fermion operators could also be generated at the loop level via e.g. a box diagram. Here we investigate the simplest scenario with a light real scalar mediator  $\phi$  with the following coupling and mass

$$\mathcal{L} \supset -\frac{1}{2}m_\phi^2\phi^2 + (g_\phi\phi\nu\nu + \text{h.c.}). \quad (3.2)$$

Here we assume that the coupling of  $\phi$  to the electron is suppressed, otherwise there would be much stronger laboratory limits.<sup>5</sup> For such neutrinophilic light mediators, UV-complete models that respect the SM gauge invariance can be built from e.g. the right-handed neutrino portal [70–73].

In the presence of the light scalar  $\phi$ , solar antineutrinos can be directly produced from

$${}^8\text{B} \rightarrow {}^8\text{Be} + e^+ + \bar{\nu} + \phi, \quad (3.3)$$

or from the subsequent decay of  $\phi$ :

$$\phi \rightarrow \nu\nu \text{ (50\%)} \text{ or } \bar{\nu}\bar{\nu} \text{ (50\%)}, \quad (3.4)$$

where the percentages indicate the branching ratios of  $\phi$  decay.

The mean distance of  $\phi$  traveling before decay is

$$\frac{\tau_\phi}{\sqrt{1-v^2}} = \frac{\tau_\phi E_\phi}{m_\phi} \sim 0.1 \text{ mm} \cdot \left(\frac{10^{-3}}{g_\phi}\right)^2 \cdot \left(\frac{\text{MeV}}{m_\phi}\right)^2 \cdot \frac{E_\phi}{10 \text{ MeV}}, \quad (3.5)$$

where  $\tau_\phi \sim 16\pi/(g_\phi^2 m_\phi)$  is the lifetime of  $\phi$  at rest. Eq. (3.5) implies that most  $\phi$  particles being produced in the Sun decay within a sub-millimeter distance. So we should include the contribution of Eq. (3.4) to the antineutrino flux.

Interestingly, when the subsequent decay of  $\phi$  is included, the solar antineutrino spectrum may exhibit the double-peak structure shown in Fig. 2, with the second peak arising from  $\phi$  decay. We find that this feature is more significant for heavier  $\phi$ . This is because the energy of  $\bar{\nu}$  produced from heavy  $\phi$  decay is generally higher than the mean energy of  $\bar{\nu}$  directly produced from  ${}^8\text{B}$  decay.

## 3.2 Results

The antineutrino flux from  ${}^8\text{B}$  decay combined with  $\phi$  decay is calculated by employing the same Monte Carlo method utilized in Sec. 2. Following similar calculations, we obtain the event rates at JUNO, HK, and THEIA. We evaluate the experimental limits on  $g_\phi$  using the same  $\chi^2$  function in Eq. (2.11) with 90% C.L., and present them in Fig. 5.

<sup>5</sup>If  $\phi$  is coupled to the electron, it would be more efficiently produced via thermal processes in the Sun and other stars, leading to very restrictive stellar cooling bounds [64–69].

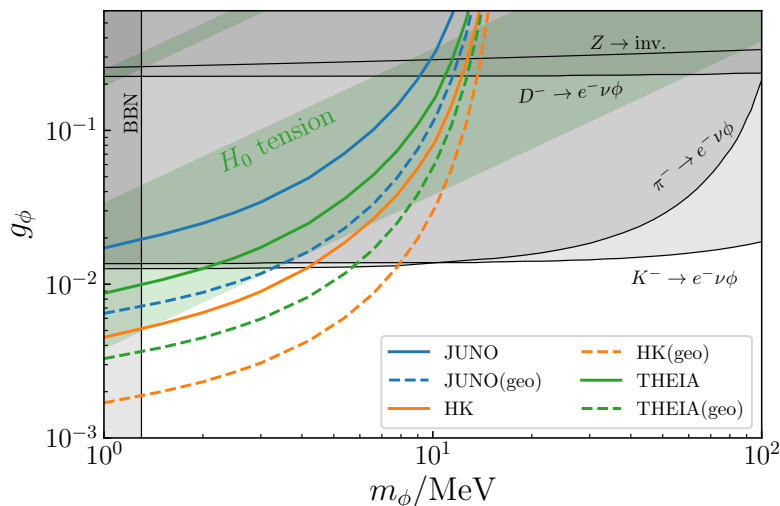


**Figure 5.** The sensitivity reach of future experiments in probing the light scalar  $\phi$  as a mediator of neutrino self-interactions, at the 90% C.L. The solid lines include reactor neutrinos and geoneutrinos as backgrounds; the dashed lines assume the reactor-off scenario, in which geoneutrinos become the dominant background.

Within the presented window, there are a few known bounds on neutrinophilic scalars, derived from meson ( $\pi^-$ ,  $K^-$ ,  $D^-$ ) decay [74],  $Z$  invisible decay [28], and Big Bang Nucleosynthesis (BBN) [27] — all have been included in Fig. 5. Compared to these known bounds, we see that solar antineutrino observations can provide the most competitive constraints on neutrinophilic scalars at the mass scale of a few MeV.

In Fig. 5, we also present two green bands on the plot, illustrating the self-interaction strengths favored by the Hubble tension — see Eq. (2.13). As is shown in the figure, when combining all existing bounds on the light scalar  $\phi$ , the region favored by the Hubble tension cannot be fully excluded, but the remaining part of the space can be probed by solar antineutrino observations.

Finally, we would like to mention the possibility that the Hubble tension may be resolved by other types of new physics or unidentified systematic errors. In this situation, our work still demonstrates that solar antineutrino observations can provide highly competitive constraints on neutrino self-interactions and also serve as a valuable complementary avenue for probing neutrino properties with cosmological significance.

## 4 Conclusion

In this paper, we have explored the potential of solar antineutrino observations as a probe of neutrino self-interactions, which could have important implications for cosmology and astrophysics. We have considered various scenarios of neutrino self-interactions including all possible Lorentz-invariant four-fermion effective operators as well as possible opening up of the effective vertices by light mediators. All these scenarios would lead to the production of solar antineutrinos.

Therefore, we present a dedicated calculation of the expected antineutrino fluxes and event rates at neutrino detectors. We find that for the self-interaction strength of cosmological interest, the resulting antineutrino fluxes will cause significant solar IBN signals at next-generation detectors like JUNO, HK, and THEIA. In particular, we have demonstrated that solar antineutrino spectra may exhibit distinctive features such as double peaks due to the presence of a light mediator.

Our results, as shown in Figs 4 and 5, imply that solar antineutrino observations can provide competitive constraints on neutrino self-interactions, and in some cases fully probe the parameter space favored by the Hubble tension. In conclusion, solar antineutrinos offer a unique opportunity to test neutrino self-interactions and might reveal unexplored features of neutrinos.

## A Identities for Weyl, Dirac, and Majorana spinors

This appendix compiles various known identities for Weyl, Dirac, and Majorana spinors. We start by briefly reviewing a few identities for anticommuting Weyl spinors  $\chi_i$  ( $i = 1, 2, 3, \dots$ ) [54]:

$$\chi_1\chi_2 = \chi_2\chi_1, \quad \chi_1^\dagger\bar{\sigma}^\mu\chi_2 = -\chi_2\sigma^\mu\chi_1^\dagger, \quad \chi_1\sigma^{\mu\nu}\chi_2 = -\chi_2\sigma^{\mu\nu}\chi_1, \quad \chi_1^\dagger\bar{\sigma}^{\mu\nu}\chi_2^\dagger = -\chi_2^\dagger\bar{\sigma}^{\mu\nu}\chi_1^\dagger, \quad (\text{A.1})$$

where  $\sigma^\mu = (1, \vec{\sigma})$ ,  $\bar{\sigma}^\mu = (1, -\vec{\sigma})$ ,  $\sigma^{\mu\nu} \equiv \frac{i}{4}(\sigma^\mu\bar{\sigma}^\nu - \sigma^\nu\bar{\sigma}^\mu)$ , and  $\bar{\sigma}^{\mu\nu} \equiv \frac{i}{4}(\bar{\sigma}^\mu\sigma^\nu - \bar{\sigma}^\nu\sigma^\mu)$ .

In addition, there are several Fierz identities [54]:

$$(\chi_1\chi_2)(\chi_3\chi_4) = -(\chi_1\chi_3)(\chi_4\chi_2) - (\chi_1\chi_4)(\chi_2\chi_3), \quad (\text{A.2})$$

$$(\chi_1^\dagger\bar{\sigma}^\mu\chi_2)(\chi_3^\dagger\bar{\sigma}_\mu\chi_4) = 2(\chi_1^\dagger\chi_3^\dagger)(\chi_4\chi_2), \quad (\text{A.3})$$

$$(\chi_1\sigma^{\mu\nu}\chi_2)(\chi_3\sigma_{\mu\nu}\chi_4) = -2(\chi_1\chi_4)(\chi_2\chi_3) - (\chi_1\chi_2)(\chi_3\chi_4), \quad (\text{A.4})$$

$$(\chi_1\sigma^{\mu\nu}\chi_2)(\chi_3^\dagger\bar{\sigma}_{\mu\nu}\chi_4^\dagger) = 0. \quad (\text{A.5})$$

Other Fierz identities not listed here are simply hermitian conjugates of the above. According to the Fierz identities, it is straightforward to see that  $\mathcal{L}_{S'}$  and  $\mathcal{L}_T$  can be transformed to  $\mathcal{L}_V$  and  $\mathcal{L}_S$ , respectively. In addition,  $\mathcal{L}_{V'}$  can also be written into the form of  $\mathcal{L}_V$  using Eq. (A.1). Therefore, only  $\mathcal{L}_S$  and  $\mathcal{L}_V$  are independent operators.

To reformulate Eqs. (2.1)-(2.5) in terms of Dirac or Majorana spinors, we define

$$\psi_D \equiv \begin{pmatrix} \nu \\ \eta^\dagger \end{pmatrix}, \quad \psi_D^c \equiv \begin{pmatrix} \eta \\ \nu^\dagger \end{pmatrix}, \quad \psi_M \equiv \begin{pmatrix} \nu \\ \nu^\dagger \end{pmatrix}. \quad (\text{A.6})$$

Here  $\eta$  denotes the Weyl spinor of a right-handed neutrino. The  $4 \times 4$  Dirac matrices are connected to  $2 \times 2$  Pauli matrices as follows:

$$\gamma^\mu = \begin{pmatrix} \sigma^\mu & \\ & \bar{\sigma}^\mu \end{pmatrix}, \quad \sigma_D^{\mu\nu} \equiv \frac{i}{2}[\gamma^\mu, \gamma^\nu] = 2 \begin{pmatrix} \sigma^{\mu\nu} & \\ & \bar{\sigma}^{\mu\nu} \end{pmatrix}. \quad (\text{A.7})$$

Using the above relations, we can reformulate Eqs. (2.1)-(2.5) in terms of Dirac spinors:

$$\mathcal{L}_S = \frac{1}{\Lambda_S^2} \overline{\psi}_D^c P_L \psi_D \overline{\psi}_D^c P_L \psi_D + \text{h.c.}, \quad (\text{A.8})$$

$$\mathcal{L}_{S'} = \frac{1}{\Lambda_{S'}^2} \overline{\psi}_D^c P_L \psi_D \overline{\psi}_D P_R \psi_D^c, \quad (\text{A.9})$$

$$\mathcal{L}_V = \frac{1}{\Lambda_V^2} (\overline{\psi}_D \gamma^\mu P_L \psi_D) (\overline{\psi}_D \gamma^\mu P_L \psi_D), \quad (\text{A.10})$$

$$\mathcal{L}_{V'} = \frac{1}{\Lambda_{V'}^2} (\overline{\psi}_D \gamma^\mu P_L \psi_D) (\overline{\psi}_D^c \gamma^\mu P_R \psi_D^c), \quad (\text{A.11})$$

$$\mathcal{L}_T = \frac{1}{\Lambda_T^2} \frac{1}{4} (\overline{\psi}_D^c \sigma_D^{\mu\nu} P_L \psi_D) (\overline{\psi}_D^c \sigma_{D\mu\nu} P_L \psi_D) + \text{h.c.} \quad (\text{A.12})$$

If using Majorana spinors, one simply needs to replace  $\psi_D \rightarrow \psi_M$  and  $\psi_D^c \rightarrow \psi_M$ . Note that for a single neutrino flavor, we have

$$\overline{\psi}_M \gamma^\mu \psi_M = 0, \quad \overline{\psi}_M \sigma_D^{\mu\nu} \psi_M = 0, \quad \overline{\psi}_M \sigma_D^{\mu\nu} \gamma^5 \psi_M = 0. \quad (\text{A.13})$$

These can be obtained using Eq. (A.1).

## B Calculation of three-body decay

In this work, we encounter a three-body decay process:  ${}^8\text{B} \rightarrow {}^8\text{Be} + e^+ + \nu_e$ . To analytically calculate this process, we assume the following effective Lagrangian:

$$\mathcal{L} \supset \frac{g_{\text{eff}}^2}{M_W^2} (\Phi_{\text{Be}}^\dagger \partial_\mu \Phi_{\text{B}}) (\overline{\psi}_\nu \gamma^\mu P_L \psi_e) + \text{h.c.}, \quad (\text{B.1})$$

where  $g_{\text{eff}}$  is a dimensionless coupling constant,  $M_W$  is the mass of  $W$  boson,  $\Phi_{\text{B}}$  and  $\Phi_{\text{Be}}$  describe  ${}^8\text{B}$  and  ${}^8\text{Be}$  as scalar fields, and  $\psi_e$  and  $\psi_\nu$  denote the Dirac spinors of  $e^\pm$  and  $\nu_e$ , respectively. Then the amplitude for  ${}^8\text{B} \rightarrow {}^8\text{Be} + e^+ + \nu_e$  reads

$$i\mathcal{M}({}^8\text{B} \rightarrow {}^8\text{Be} + e^+ + \nu_e) = \frac{g_{\text{eff}}^2}{M_W^2} \overline{u}_3 \not{p} P_L v_2. \quad (\text{B.2})$$

where  $p$  denotes the momentum of  ${}^8\text{B}$ ;  $u_3$  and  $v_2$  denote the final states of  $\nu_e$  and  $e^+$  respectively.

The amplitude squared, after applying the spin summation, reads

$$\begin{aligned} |\mathcal{M}({}^8\text{B} \rightarrow {}^8\text{Be} + e^+ + \nu_e)|^2 &= \frac{g_{\text{eff}}^2}{M_W^4} \text{tr}[\not{p}_3 \not{p} P_L (\not{p}_2 - m_e) \not{p} P_L] \\ &= \frac{g_{\text{eff}}^2}{M_W^4} [4(p_2 \cdot p)(p_3 \cdot p) - 2(p_2 \cdot p_3)p^2] \\ &= \frac{2g_{\text{eff}}^2 M^2}{M_W^4} E_2 E_3 (1 + \cos \theta_{23}), \end{aligned} \quad (\text{B.3})$$

where  $p_1$ ,  $p_2$ , and  $p_3$  denote the four-momenta of  ${}^8\text{Be}$ ,  $e^+$ , and  $\nu_e$ , respectively.  $M$  denotes the mass of  ${}^8\text{B}$ .

Next, we shall compute the three-body phase integration, which reads

$$\begin{aligned}
\int d\Phi_n(p; p_1, p_2, p_3) &\equiv \int \frac{d^3\mathbf{p}_1}{(2\pi)^3 2E_1} \frac{d^3\mathbf{p}_2}{(2\pi)^3 2E_2} \frac{d^3\mathbf{p}_3}{(2\pi)^3 2E_3} (2\pi)^4 \delta^{(4)}(p - p_1 - p_2 - p_3) \\
&= \frac{1}{8(2\pi)^5} \int \frac{d^3\mathbf{p}_2 d^3\mathbf{p}_3}{E_1 E_2 E_3} \delta(E_p - E_1 - E_2 - E_3) \\
&= \frac{1}{8(2\pi)^5} \int \frac{E_2^2 dE_2 E_3^2 dE_3}{E_1 E_2 E_3} d\Omega_2 d\Omega_3 \delta(E_p - E_1 - E_2 - E_3) \\
&= \frac{1}{4(2\pi)^4} \int \frac{E_2 E_3}{E_1} dE_2 dE_3 d\phi_{23} d\cos\theta_{23} \delta(E_p - E_1 - E_2 - E_3) \\
&= \frac{1}{4(2\pi)^3} \int dE_2 dE_3 d\cos\theta_{23} \delta(E_p - E_1 - E_2 - E_3) \frac{E_2 E_3}{E_1}.
\end{aligned} \tag{B.4}$$

Applying the above to  ${}^8\text{B}$  decay at rest, we obtain

$$\begin{aligned}
\Gamma &= \frac{1}{2M} \int d\Phi_n(q; k_1, k_2, k_3) \overline{\sum} |\mathcal{M}|^2 \\
&= \frac{g_{\text{eff}}^2 M}{4(2\pi)^3 M_W^4} \int dE_2 dE_3 d\cos\theta_{23} \delta(M - E_1 - E_2 - E_3) \frac{E_2^2 E_3^2}{E_1} (1 + \cos\theta_{23}) \\
&= \frac{g_{\text{eff}}^2 M}{8(2\pi)^3 M_W^4} \int dE_2 dE_3 [M^2 - M'^2 - 2M(E_2 + E_3) + 4E_2 E_3],
\end{aligned} \tag{B.5}$$

where  $M'$  is the mass of  ${}^8\text{Be}$  and we have used

$$\begin{aligned}
1 + \cos\theta_{23} &= 1 + \frac{(M - E_2 - E_3)^2 - M'^2 - E_2^2 - E_3^2}{2E_2 E_3} \\
&= \frac{M^2 - M'^2 - 2M(E_2 + E_3) + 4E_2 E_3}{2E_2 E_3},
\end{aligned} \tag{B.6}$$

$$\left| \frac{\partial(M - E_1 - E_2 - E_3)}{\partial \cos\theta_{23}} \right| = \frac{E_2 E_3}{E_1}, \tag{B.7}$$

which are derived from

$$M - E_2 - E_3 = E_1 = \sqrt{M'^2 + E_2^2 + E_3^2 + 2E_2 E_3 \cos\theta_{23}}. \tag{B.8}$$

The differential decay rate is given by

$$\frac{d\Gamma}{dE_3} = \frac{g_{\text{eff}}^2 M}{8(2\pi)^3 M_W^4} \int_{E_2^{\min}(E_3)}^{E_2^{\max}(E_3)} dE_2 [M^2 - M'^2 - 2M(E_2 + E_3) + 4E_2 E_3], \tag{B.9}$$

where

$$E_2(E_3, \cos\theta) = \frac{M(M - 2E_3) - M'^2}{2[M - E_3(1 - \cos\theta_{23})]}. \tag{B.10}$$

It has the following upper and lower bounds:

$$E_2^{\min}(E_3) = \frac{M(M - 2E_3) - M'^2}{2M}, \tag{B.11}$$

$$E_2^{\max}(E_3) = \frac{M(M - 2E_3) - M'^2}{2(M - 2E_3)}. \tag{B.12}$$

Integrating out  $E_2$  in Eq. (B.9), we obtain

$$\frac{d\Gamma}{dE_3} = \frac{g_{\text{eff}}^2}{8(2\pi)^3 M_W^4} \frac{E_3^2 [M(M - 2E_3) - M'^2]^2}{M(M - 2E_3)}, \quad (\text{B.13})$$

where  $E_3 \in [0, (M^2 - M'^2)/(2M)]$ .

Further integrating out  $E_3$ , we obtain the total decay rate:

$$\Gamma = \frac{g_{\text{eff}}^2}{8(2\pi)^3 M_W^4} \frac{1}{96M^3} \left[ M^8 - 8M^6 M'^2 + 24M^4 M'^4 \ln \frac{M}{M'} + 8M^2 M'^6 - M'^8 \right]. \quad (\text{B.14})$$

## C Calculation of four- and five-body decay

For  ${}^8\text{B} \rightarrow {}^8\text{Be} + e^+ + \bar{\nu} + \phi$  and  ${}^8\text{B} \rightarrow {}^8\text{Be} + e^+ + 3\nu(\bar{\nu})$ , we need to compute four- and five-body phase space integrals. The practical way of handling with such phase space integrals is to adopt the time-like recursion relations [55], which will be briefly reviewed below.

In general, an  $n$ -body decay rate reads

$$d\Gamma = \frac{1}{S} \frac{1}{2M} |\mathcal{M}|^2 d\Phi_n, \quad (\text{C.1})$$

where  $S$  is the *symmetry factor* accounting for identical particles,  $M$  is the mass of the initial particle,  $\mathcal{M}$  is the amplitude of the decay process, and  $d\Phi_n$  is given by

$$d\Phi_n = (2\pi)^4 \delta^{(4)} \left( p - \sum_{i=1}^n p_i \right) \prod_{i=1}^n \frac{d^3 \mathbf{p}_i}{(2\pi)^3 2E_i}. \quad (\text{C.2})$$

The phase space can be written recursively as

$$\begin{aligned} d\Phi_n &= \frac{d^3 \mathbf{p}_n}{(2\pi)^3 2E_n} \left( \prod_{i=1}^{n-1} \frac{d^3 \mathbf{p}_i}{(2\pi)^3 2E_i} \right) (2\pi)^4 \left( (p - p_n) - \sum_{i=1}^{n-1} p_i \right) \\ &= \frac{d^3 \mathbf{p}_n}{(2\pi)^3 2E_n} d\Phi_{n-1}(p - p_n; p_1, \dots, p_{n-1}). \end{aligned} \quad (\text{C.3})$$

Let us define

$$k_i \equiv \sum_{j=1}^i p_j, \quad M_i^2 \equiv k_i^2, \quad (\text{C.4})$$

then we can insert the following integrals

$$1 \equiv \int dM_{n-1}^2 \delta(k_{n-1}^2 - M_{n-1}^2), \quad (\text{C.5})$$

$$1 \equiv \int d^4 k_{n-1} \delta^{(4)}(p - p_n - k_{n-1}) \quad (\text{C.6})$$

into Eq. (C.3) and obtain

$$\begin{aligned}
\int d\Phi_n &= \int_{\mu_{n-1}^2}^{(M_n-m_n)^2} \frac{dM_{n-1}^2}{2\pi} \\
&\quad \times \int \frac{d^4 k_{n-1}}{(2\pi)^4} \frac{d^4 p_n}{(2\pi)^4} (2\pi)^4 \delta^{(4)}(p-p_n-k_{n-1}) 2\pi \delta(k_{n-1}^2 - M_{n-1}^2) 2\pi \delta(p_n^2 - m_n^2) \\
&\quad \times \int d\Phi_{n-1}(p-p_n; p_1, \dots, p_{n-1}) \\
&= \int_{\mu_{n-1}^2}^{(M_n-m_n)^2} \frac{dM_{n-1}^2}{2\pi} \int d\Phi_2(k_n; k_{n-1}, p_n) d\Phi_{n-1}(p-p_n; p_1, \dots, p_{n-1}) \\
&= \int_{\mu_{n-1}^2}^{(M_n-m_n)^2} \frac{dM_{n-1}^2}{2\pi} \int \frac{d\Omega_{n-1}}{(2\pi)^2} \frac{\sqrt{\lambda(M_n^2, M_{n-1}^2, m_n^2)}}{8M_n^2} \\
&\quad \times \int d\Phi_{n-1}(p-p_n; p_1, \dots, p_{n-1}).
\end{aligned} \tag{C.7}$$

where  $\mu_i \equiv \sum_{j=1}^i m_j$ ,  $m_i^2 \equiv p_i^2$ , and  $d\Omega_i$  is defined as the differential solid angle in the rest frame of  $k_{i+1}$ , i.e.,  $\mathbf{k}_{i+1} = 0$ .

So the final result is

$$\int d\Phi_n = \frac{1}{(2\pi)^{3n-4}} \int_{\mu_{n-1}}^{M_n-m_n} dM_{n-1} \cdots \int_{\mu_2}^{M_3-m_3} dM_2 \left( \int \prod_{i=1}^{n-1} d\Omega_i \right) \frac{1}{2^n M_n} \prod_{i=2}^n P_i, \tag{C.8}$$

where

$$P_i \equiv \frac{\sqrt{\lambda(M_i^2, M_{i-1}^2, m_i^2)}}{2M_i}, \tag{C.9}$$

$$\lambda(x, y, z) \equiv (x - y - z)^2 - 4yz. \tag{C.10}$$

Substituting Eq. (C.8) into Eq. (C.1), we can perform Monte Carlo integration straightforwardly, provided that  $|\mathcal{M}|^2$  is known. For those four- or five-body processes considered in this work,  $|\mathcal{M}|^2$  can be computed analytically assuming the interaction in Eq. (B.1). The results for the four-fermion operators are

$$|\mathcal{M}_S|^2 = \frac{g_{\text{eff}}^2}{M_W^4} \frac{4p_4 \cdot p_5}{\Lambda_S^2 q^4} (M^2 (p_2 \cdot p_3 q^2 - 2q \cdot p_2 q \cdot p_3) + 2p \cdot p_2 (2p \cdot q q \cdot p_3 - p \cdot p_3 q^2)), \tag{C.11}$$

$$|\mathcal{M}_V|^2 = \frac{g_{\text{eff}}^2}{M_W^4} \frac{16p_3 \cdot p_4}{\Lambda_V^2 q^4} (M^2 (p_2 \cdot p_5 q^2 - 2q \cdot p_2 q \cdot p_5) + 2p \cdot p_2 (2p \cdot q q \cdot p_5 - p \cdot p_5 q^2)), \tag{C.12}$$

$$|\mathcal{M}_T|^2 = 64 \frac{g_{\text{eff}}^2}{M_W^4} \frac{2p_3 \cdot p_5}{q^4} (M^2 (p_2 \cdot p_4 q^2 - 2q \cdot p_2 q \cdot p_4) + p \cdot p_2 (4p \cdot q q \cdot p_4 - 2p \cdot p_4 q^2)) \tag{C.13}$$

$$+ 64 \frac{g_{\text{eff}}^2}{M_W^4} \frac{2p_3 \cdot p_4}{q^4} (M^2 (p_2 \cdot p_5 q^2 - 2q \cdot p_2 q \cdot p_5) + p \cdot p_2 (4p \cdot q q \cdot p_5 - 2p \cdot p_5 q^2)) \tag{C.14}$$

$$+ 64 \frac{g_{\text{eff}}^2}{M_W^4} \frac{p_4 \cdot p_5}{q^4} (M^2 (2q \cdot p_2 q \cdot p_3 - p_2 \cdot p_3 q^2) + 2p \cdot p_2 (p \cdot p_3 q^2 - 2p \cdot q q \cdot p_3)), \tag{C.15}$$



where the subscripts  $S$ ,  $V$ ,  $T$  indicate the type of the four-fermion operators used. For  $S'$  and  $V'$  operators, the results can be simply obtained via  $\mathcal{M}_{S'} = \mathcal{M}_S|_{\Lambda_s \rightarrow \Lambda_{s'}}$ ,  $\mathcal{M}_{V'} = \mathcal{M}_V|_{\Lambda_V \rightarrow \Lambda_{V'}}$ .

For the scalar mediator in Eq. (3.2), the squared amplitude of  ${}^8\text{B} \rightarrow {}^8\text{Be} + e^+ + \bar{\nu} + \phi$  is given by

$$|\mathcal{M}_\phi|^2 = \frac{g_{\text{eff}}^2}{M_W^4} \frac{g_\phi^2}{q^4} (2M^2 (p_2 \cdot p_3 q^2 - 2q \cdot p_2 q \cdot p_3) + p \cdot p_2 (8p \cdot q q \cdot p_3 - 4p \cdot p_3 q^2)), \quad (\text{C.16})$$

where  $q = p_3 + p_4$  with  $p_3$  and  $p_4$  denoting the momenta of  $\bar{\nu}$  and  $\phi$ , respectively.

## Acknowledgments

We acknowledge the use of FEYN CALC [75–77] and PACKAGE X [78, 79] in this work. X.-J. Xu is supported in part by the National Natural Science Foundation of China under grant No. 12141501 and also by the CAS Project for Young Scientists in Basic Research (YSBR-099). Q.-f. Wu is supported by the National Natural Science Foundation of China under grant No. 12075251.

## References

- [1] M. Maltoni and A. Y. Smirnov, *Solar neutrinos and neutrino physics*, *Eur. Phys. J. A* **52** (2016), no. 4 87, [[1507.05287](#)].
- [2] X.-J. Xu, Z. Wang, and S. Chen, *Solar neutrino physics*, *Prog. Part. Nucl. Phys.* **131** (2023) 104043, [[2209.14832](#)].
- [3] **Super-Kamiokande Collaboration**, Y. Gando *et al.*, *Search for anti- $\nu(e)$  from the sun at Super-Kamiokande I*, *Phys. Rev. Lett.* **90** (2003) 171302, [[hep-ex/0212067](#)].
- [4] **SNO Collaboration**, B. Aharmim *et al.*, *Electron antineutrino search at the Sudbury Neutrino Observatory*, *Phys. Rev. D* **70** (2004) 093014, [[hep-ex/0407029](#)].
- [5] **KamLAND Collaboration**, A. Gando *et al.*, *A study of extraterrestrial antineutrino sources with the KamLAND detector*, *Astrophys. J.* **745** (2012) 193, [[1105.3516](#)].
- [6] **Borexino Collaboration**, M. Agostini *et al.*, *Search for low-energy neutrinos from astrophysical sources with Borexino*, *Astropart. Phys.* **125** (2021) 102509, [[1909.02422](#)].
- [7] **KamLAND Collaboration**, S. Abe *et al.*, *Limits on Astrophysical Antineutrinos with the KamLAND Experiment*, *Astrophys. J.* **925** (2022), no. 1 14, [[2108.08527](#)].
- [8] **Super-Kamiokande Collaboration**, K. Abe *et al.*, *Search for solar electron anti-neutrinos due to spin-flavor precession in the Sun with Super-Kamiokande-IV*, *Astropart. Phys.* **139** (2022) 102702, [[2012.03807](#)].
- [9] B. Pontecorvo, *Mesonium and anti-mesonium*, *Sov. Phys. JETP* **6** (1957) 429.
- [10] B. Pontecorvo, *Inverse beta processes and nonconservation of lepton charge*, *Zh. Eksp. Teor. Fiz.* **34** (1957) 247.
- [11] R. Davis, Jr., D. S. Harmer, and K. C. Hoffman, *Search for neutrinos from the sun*, *Phys. Rev. Lett.* **20** (1968) 1205–1209.

- [12] J. N. Bahcall, N. A. Bahcall, and G. Shaviv, *Present status of the theoretical predictions for the Cl-36 solar neutrino experiment*, *Phys. Rev. Lett.* **20** (1968) 1209–1212.
- [13] A. Cisneros, *Effect of neutrino magnetic moment on solar neutrino observations*, *Astrophys. Space Sci.* **10** (1971) 87–92.
- [14] L. B. Okun, M. B. Voloshin, and M. I. Vysotsky, *Neutrino electrodynamics and possible effects for solar neutrinos*, *Sov. Phys. JETP* **64** (1986) 446–452.
- [15] C.-S. Lim and W. J. Marciano, *Resonant Spin - Flavor Precession of Solar and Supernova Neutrinos*, *Phys. Rev. D* **37** (1988) 1368–1373.
- [16] E. K. Akhmedov, *Resonant Amplification of Neutrino Spin Rotation in Matter and the Solar Neutrino Problem*, *Phys. Lett. B* **213** (1988) 64–68.
- [17] E. K. Akhmedov and J. Pulido, *Solar neutrino oscillations and bounds on neutrino magnetic moment and solar magnetic field*, *Phys. Lett. B* **553** (2003) 7–17, [[hep-ph/0209192](#)].
- [18] E. Akhmedov and P. Martínez-Miravé, *Solar  $\bar{\nu}_e$  flux: revisiting bounds on neutrino magnetic moments and solar magnetic field*, *JHEP* **10** (2022) 144, [[2207.04516](#)].
- [19] J. F. Beacom and N. F. Bell, *Do Solar Neutrinos Decay?*, *Phys. Rev. D* **65** (2002) 113009, [[hep-ph/0204111](#)].
- [20] R. Lehnert and T. J. Weiler, *Neutrino flavor ratios as diagnostic of solar WIMP annihilation*, *Phys. Rev. D* **77** (2008) 125004, [[0708.1035](#)].
- [21] C. Rott, J. Siegal-Gaskins, and J. F. Beacom, *New Sensitivity to Solar WIMP Annihilation using Low-Energy Neutrinos*, *Phys. Rev. D* **88** (2013) 055005, [[1208.0827](#)].
- [22] N. Bernal, J. Martín-Albo, and S. Palomares-Ruiz, *A novel way of constraining WIMPs annihilations in the Sun: MeV neutrinos*, *JCAP* **08** (2013) 011, [[1208.0834](#)].
- [23] W.-L. Guo, *Detecting electron neutrinos from solar dark matter annihilation by JUNO*, *JCAP* **01** (2016) 039, [[1511.04888](#)].
- [24] L. Funcke, G. Raffelt, and E. Vitagliano, *Distinguishing Dirac and Majorana neutrinos by their decays via Nambu-Goldstone bosons in the gravitational-anomaly model of neutrino masses*, *Phys. Rev. D* **101** (2020), no. 1 015025, [[1905.01264](#)].
- [25] M. Hostert and M. Pospelov, *Constraints on decaying sterile neutrinos from solar antineutrinos*, *Phys. Rev. D* **104** (2021), no. 5 055031, [[2008.11851](#)].
- [26] R. Picoreti, D. Pramanik, P. C. de Holanda, and O. L. G. Peres, *Updating  $\nu_3$  lifetime from solar antineutrino spectra*, *Phys. Rev. D* **106** (2022), no. 1 015025, [[2109.13272](#)].
- [27] N. Blinov, K. J. Kelly, G. Z. Krnjaic, and S. D. McDermott, *Constraining the Self-Interacting Neutrino Interpretation of the Hubble Tension*, *Phys. Rev. Lett.* **123** (2019), no. 19 191102, [[1905.02727](#)].
- [28] V. Brdar, M. Lindner, S. Vogl, and X.-J. Xu, *Revisiting neutrino self-interaction constraints from Z and  $\tau$  decays*, *Phys. Rev. D* **101** (2020), no. 11 115001, [[2003.05339](#)].
- [29] F. F. Deppisch, L. Graf, W. Rodejohann, and X.-J. Xu, *Neutrino Self-Interactions and Double Beta Decay*, *Phys. Rev. D* **102** (2020), no. 5 051701, [[2004.11919](#)].
- [30] J. M. Berryman *et al.*, *Neutrino self-interactions: A white paper*, *Phys. Dark Univ.* **42** (2023) 101267, [[2203.01955](#)].

- [31] C. D. Kreisch, F.-Y. Cyr-Racine, and O. Doré, *Neutrino puzzle: Anomalies, interactions, and cosmological tensions*, *Phys. Rev. D* **101** (2020), no. 12 123505, [[1902.00534](#)].
- [32] A. Das, Y. F. Perez-Gonzalez, and M. Sen, *Neutrino secret self-interactions: A booster shot for the cosmic neutrino background*, *Phys. Rev. D* **106** (2022), no. 9 095042, [[2204.11885](#)].
- [33] M. Bustamante, C. Rosenstrøm, S. Shalgar, and I. Tamborra, *Bounds on secret neutrino interactions from high-energy astrophysical neutrinos*, *Phys. Rev. D* **101** (2020), no. 12 123024, [[2001.04994](#)].
- [34] P.-W. Chang, I. Esteban, J. F. Beacom, T. A. Thompson, and C. M. Hirata, *Towards Powerful Probes of Neutrino Self-Interactions in Supernovae*, [2206.12426](#).
- [35] J. Venzor, G. Garcia-Arroyo, A. Pérez-Lorenzana, and J. De-Santiago, *Massive neutrino self-interactions with a light mediator in cosmology*, *Phys. Rev. D* **105** (2022), no. 12 123539, [[2202.09310](#)].
- [36] J. Venzor, G. Garcia-Arroyo, A. Pérez-Lorenzana, and J. De-Santiago, *Resonant neutrino self-interactions and the  $H_0$  tension*, [2303.12792](#).
- [37] I. Esteban, S. Pandey, V. Brdar, and J. F. Beacom, *Probing secret interactions of astrophysical neutrinos in the high-statistics era*, *Phys. Rev. D* **104** (2021), no. 12 123014, [[2107.13568](#)].
- [38] D. F. G. Fiorillo, G. Raffelt, and E. Vitagliano, *Supernova Emission of Secretly Interacting Neutrino Fluid: Theoretical Foundations*, [2307.15122](#).
- [39] D. F. G. Fiorillo, G. Raffelt, and E. Vitagliano, *Large Neutrino Secret Interactions, Small Impact on Supernovae*, [2307.15115](#).
- [40] S.-P. Li and X.-J. Xu,  *$N_{eff}$  constraints on light mediators coupled to neutrinos: the dilution-resistant effect*, *JHEP* **10** (2023) 012, [[2307.13967](#)].
- [41] S. Roy Choudhury, S. Hannestad, and T. Tram, *Updated constraints on massive neutrino self-interactions from cosmology in light of the  $H_0$  tension*, *JCAP* **03** (2021) 084, [[2012.07519](#)].
- [42] S. Roy Choudhury, S. Hannestad, and T. Tram, *Massive neutrino self-interactions and inflation*, *JCAP* **10** (2022) 018, [[2207.07142](#)].
- [43] K. Ioka and K. Murase, *IceCube PeV–EeV neutrinos and secret interactions of neutrinos*, *PTEP* **2014** (2014), no. 6 061E01, [[1404.2279](#)].
- [44] K. Blum, A. Hook, and K. Murase, *High energy neutrino telescopes as a probe of the neutrino mass mechanism*, [1408.3799](#).
- [45] I. M. Shoemaker and K. Murase, *Probing BSM Neutrino Physics with Flavor and Spectral Distortions: Prospects for Future High-Energy Neutrino Telescopes*, *Phys. Rev. D* **93** (2016), no. 8 085004, [[1512.07228](#)].
- [46] J. A. Carpio, K. Murase, I. M. Shoemaker, and Z. Tabrizi, *High-energy cosmic neutrinos as a probe of the vector mediator scenario in light of the muon  $g-2$  anomaly and Hubble tension*, *Phys. Rev. D* **107** (2023), no. 10 103057, [[2104.15136](#)].
- [47] Y. Chen, X. Xue, and V. Cardoso, *Black Holes as Neutrino Factories*, [2308.00741](#).
- [48] G. Barenboim, P. B. Denton, and I. M. Oldengott, *Constraints on inflation with an extended neutrino sector*, *Phys. Rev. D* **99** (2019), no. 8 083515, [[1903.02036](#)].

- [49] **JUNO Collaboration**, F. An *et al.*, *Neutrino Physics with JUNO*, *J. Phys. G* **43** (2016), no. 3 030401, [[1507.05613](#)].
- [50] **Hyper-Kamiokande Collaboration**, K. Abe *et al.*, *Hyper-Kamiokande Design Report*, [1805.04163](#).
- [51] **Theia Collaboration**, M. Askins *et al.*, *THEIA: an advanced optical neutrino detector*, *Eur. Phys. J. C* **80** (2020), no. 5 416, [[1911.03501](#)].
- [52] X. Luo, W. Rodejohann, and X.-J. Xu, *Dirac neutrinos and  $N_{\text{eff}}$* , *JCAP* **06** (2020) 058, [[2005.01629](#)].
- [53] X. Luo, W. Rodejohann, and X.-J. Xu, *Dirac neutrinos and  $N_{\text{eff}}$ . Part II. The freeze-in case*, *JCAP* **03** (2021) 082, [[2011.13059](#)].
- [54] H. K. Dreiner, H. E. Haber, and S. P. Martin, *Two-component spinor techniques and Feynman rules for quantum field theory and supersymmetry*, *Phys. Rept.* **494** (2010) 1–196, [[0812.1594](#)].
- [55] E. Byckling and K. Kajantie, *Particle Kinematics*. A Wiley-Interscience publication. Wiley, 1973.
- [56] <http://www.nu-fit.org>.
- [57] I. Esteban, M. C. Gonzalez-Garcia, M. Maltoni, T. Schwetz, and A. Zhou, *The fate of hints: updated global analysis of three-flavor neutrino oscillations*, *JHEP* **09** (2020) 178, [[2007.14792](#)].
- [58] V. Brdar and X.-J. Xu, *Beyond tree level with solar neutrinos: Towards measuring the flavor composition and CP violation*, *Phys. Lett. B* **846** (2023) 138255, [[2306.03160](#)].
- [59] A. Strumia and F. Vissani, *Precise quasielastic neutrino/nucleon cross-section*, *Phys. Lett. B* **564** (2003) 42–54, [[astro-ph/0302055](#)].
- [60] **Particle Data Group Collaboration**, P. A. Zyla *et al.*, *Review of Particle Physics*, *PTEP* **2020** (2020), no. 8 083C01.
- [61] V. I. Kopeikin, *Flux and spectrum of reactor antineutrinos*, *Phys. Atom. Nucl.* **75** (2012) 143–152.
- [62] **JUNO Collaboration**, A. Abusleme *et al.*, *Juno physics and detector*, *Prog. Part. Nucl. Phys.* **123** (2022) 103927, [[2104.02565](#)].
- [63] **Borexino Collaboration**, M. Agostini *et al.*, *Comprehensive geoneutrino analysis with borexino*, *Phys. Rev. D* **101** (2020), no. 1 012009, [[1909.02257](#)].
- [64] J. Redondo, *Helioscope Bounds on Hidden Sector Photons*, *JCAP* **07** (2008) 008, [[0801.1527](#)].
- [65] H. An, M. Pospelov, and J. Pradler, *New stellar constraints on dark photons*, *Phys. Lett. B* **725** (2013) 190–195, [[1302.3884](#)].
- [66] J. Redondo and G. Raffelt, *Solar constraints on hidden photons re-visited*, *JCAP* **08** (2013) 034, [[1305.2920](#)].
- [67] N. Vinyoles, A. Serenelli, F. L. Villante, S. Basu, J. Redondo, and J. Isern, *New axion and hidden photon constraints from a solar data global fit*, *JCAP* **10** (2015) 015, [[1501.01639](#)].
- [68] H. An, M. Pospelov, J. Pradler, and A. Ritz, *New limits on dark photons from solar emission and keV scale dark matter*, *Phys. Rev. D* **102** (2020) 115022, [[2006.13929](#)].

- [69] S.-P. Li and X.-J. Xu, *Production rates of dark photons and  $Z'$  in the Sun and stellar cooling bounds*, *JCAP* **09** (2023) 009, [[2304.12907](#)].
- [70] M. Berbig, S. Jana, and A. Trautner, *The Hubble tension and a renormalizable model of gauged neutrino self-interactions*, *Phys. Rev. D* **102** (2020), no. 11 115008, [[2004.13039](#)].
- [71] X.-J. Xu, *The  $\nu_R$ -philic scalar: its loop-induced interactions and Yukawa forces in LIGO observations*, *JHEP* **09** (2020) 105, [[2007.01893](#)].
- [72] G. Chauhan and X.-J. Xu, *How dark is the  $\nu_R$ -philic dark photon?*, *JHEP* **04** (2021) 003, [[2012.09980](#)].
- [73] G. Chauhan, P. S. B. Dev, and X.-J. Xu, *Probing the  $\nu_R$ -philic  $Z'$  at DUNE near detectors*, *Phys. Lett. B* **841** (2023) 137907, [[2204.11876](#)].
- [74] J. M. Berryman, A. De Gouvêa, K. J. Kelly, and Y. Zhang, *Lepton-Number-Charged Scalars and Neutrino Beamstrahlung*, *Phys. Rev. D* **97** (2018), no. 7 075030, [[1802.00009](#)].
- [75] R. Mertig, M. Bohm, and A. Denner, *FEYN CALC: Computer algebraic calculation of Feynman amplitudes*, *Comput. Phys. Commun.* **64** (1991) 345–359.
- [76] V. Shtabovenko, R. Mertig, and F. Orellana, *New Developments in FeynCalc 9.0*, *Comput. Phys. Commun.* **207** (2016) 432–444, [[1601.01167](#)].
- [77] V. Shtabovenko, R. Mertig, and F. Orellana, *FeynCalc 9.3: New features and improvements*, *Comput. Phys. Commun.* **256** (2020) 107478, [[2001.04407](#)].
- [78] H. H. Patel, *Package-X: A Mathematica package for the analytic calculation of one-loop integrals*, *Comput. Phys. Commun.* **197** (2015) 276–290, [[1503.01469](#)].
- [79] H. H. Patel, *Package-X 2.0: A Mathematica package for the analytic calculation of one-loop integrals*, *Comput. Phys. Commun.* **218** (2017) 66–70, [[1612.00009](#)].